Computer Assisted Methods in Engineering and Science, **19**: 393–402, 2012.

Numerical procedure of solving some inverse problem in solidification of the binary alloy

Edyta Hetmaniok, Damian Słota
Institute of Mathematics, Silesian University of Technology
Kaszubska 23, 44-100 Gliwice
e-mail: damian.slota@polsl.pl

The paper presents a solution of an inverse problem consisting in determination of boundary conditions in the process of binary alloy solidification when temperature measurements in selected points of the cast are known. In the investigated model the distribution of temperature is described using the Stefan model with the liquidus temperature varying in dependance on concentration of the alloy component. For description of the concentration we apply the model in which the immediate equalization of chemical composition of the alloy is assumed (lever arm model). Experimental verification of the developed algorithm is also presented.

Keywords: solidification, segregation, binary alloy, genetic algorithm.

1. Introduction

The process of alloy solidification depends on segregation of the alloy components. For example, together with the change of concentration also the liquidus and solidus temperatures change [5, 10]. The macrosegregation problem and the problem of binary alloy solidification are analyzed in, among others, [2, 9, 12–14, 16–21, 26–31, 34]. In some of these works concentration is described using models in which the immediate equalization of chemical composition of the alloy in liquid phase and solid phase is assumed (lever arm model) [14, 16, 34], as well as the Scheil model [14, 16, 17] and the broken line model [14, 16, 28].

In the majority of available papers concerning these topics direct problems are discussed. The inverse problem applied for the binary alloy solidification is investigated in papers [6, 7, 20, 33]. The model considered in all these works is based on the Stefan problem and the macrosegregation is modeled on the assumption that in the solid phase there is no diffusion of the alloy component.

In the model developed in the current paper the distribution of temperature is described using the Stefan problem [3, 8, 15] with varying temperature of solidification depending on concentration of the alloy component. Concentration is described by means of the model in which the immediate equalization of chemical composition of the alloy in the liquid phase and solid phase is assumed (lever arm model) [1, 14]. The problem discussed in the current paper consists in determination of the heat transfer coefficient on the domain boundary when temperature measurements in selected points of the cast are known.

2. Formulation of the problem

In region Ω taken by the solidifying material two subregions Ω_1 and Ω_2 varying in time are analyzed (see Fig. 1). These regions are separated by a boundary Γ_g determined by the liquidus temperature

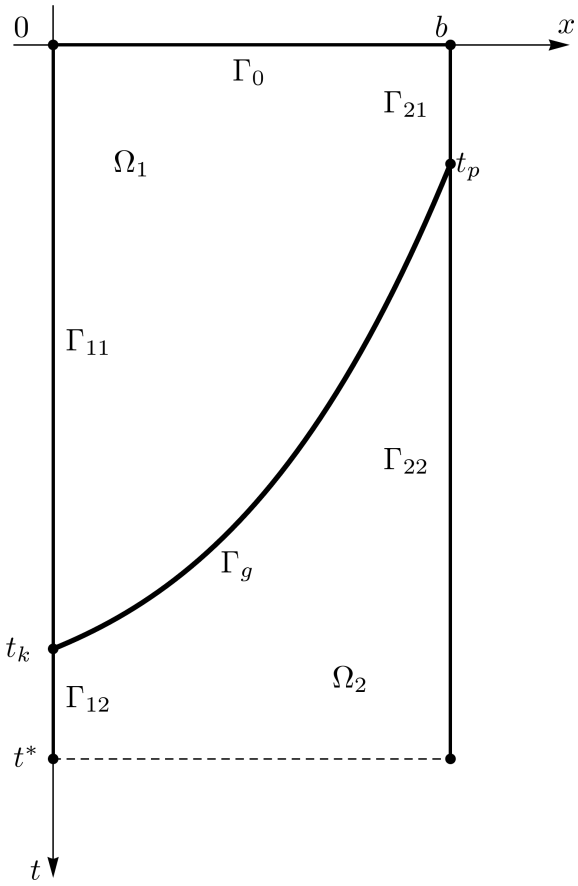

Fig. 1. Region of the problem.

varying in time (or by the so-called substitute temperature of solidification [15]). Distribution of temperature T_i in each subregion is described by means of the heat conduction equation ($i = 1, 2$):

$$c_i \, \varrho_i \, \frac{\partial T_i}{\partial t}(x,t) = \lambda_i \, \frac{\partial^2 T_i}{\partial x^2}(x,t), \tag{1}$$

for $x \in \Omega_i$, $t \in (0, t^*)$, where c_i, ϱ_i and λ_i denote the specific heat, mass density and thermal conductivity, while t and x refer to the time and spatial location, respectively.

On boundary Γ_0 the initial condition is given ($T_0 > T^*(Z_0)$):

$$T_1(x,0) = T_0, \tag{2}$$

where T_0 is the initial temperature, T^* is the liquidus temperature varying in time and Z_0 is the initial concentration of alloy component.

On boundaries Γ_{1i} ($i = 1, 2$) the homogeneous boundary conditions of the second kind are determined

$$\frac{\partial T_i}{\partial x}(0,t) = 0, \tag{3}$$

whereas, on boundaries Γ_{2i} ($i = 1, 2$) the boundary conditions of the third kind are given

$$-\lambda_i \, \frac{\partial T_i}{\partial x}(b,t) = \alpha(t) \left(T_i(b,t) - T_\infty \right), \tag{4}$$

where $\alpha(t)$ is the heat transfer coefficient and T_∞ denotes the ambient temperature.

On boundary Γ_g the condition of temperature continuity and the Stefan condition are assumed

$$T_1\big(\xi(t),t\big) = T_2\big(\xi(t),t\big) = T^*\big(Z_L(t)\big), \tag{5}$$

$$L\,\varrho_2\,\frac{d\xi(t)}{dt} = -\lambda_1 \frac{\partial T_1(x,t)}{\partial x}\bigg|_{x=\xi(t)} + \lambda_2 \frac{\partial T_2(x,t)}{\partial x}\bigg|_{x=\xi(t)}, \tag{6}$$

where T^* is the liquidus temperature, $Z_L(t)$ is the concentration of alloy component in the interface on the liquid phase side, L is the latent heat of fusion and $\xi(t)$ refers to the function describing the interface location.

The macrosegregation process, taking place in casting, is described using the model in which the immediate equalization of chemical composition of the alloy in the liquid phase and solid phase is assumed (lever arm model) [14]. Therefore we assume that $D_i \to \infty$, for $i = 1, 2$, where D_1 and D_2 denote the diffusion coefficients in liquid phase and solid phase, respectively.

Let us discretize interval $[0, t^*]$ with the nodes t_i, $i = 0, 1, \ldots, p^*$. Next, using the mass balance of alloy component in the region of cast for the moment of time t_{p+1} we obtain the following equation

$$m_0\, Z_0 = m_L(t_{p+1})\, Z_L(t_{p+1}) + m_S(t_{p+1})\, Z_S(t_{p+1}), \tag{7}$$

where m_0 denotes the mass of alloy, Z_0 is the initial concentration of alloy component, $Z_L(t_{p+1})$ and $Z_S(t_{p+1})$ refer to the concentration of alloy component in the liquid phase and solid phase at moment t_{p+1}, $m_L(t_{p+1})$ and $m_S(t_{p+1})$ denote the mass of alloy in the liquid state and solid state at moment t_{p+1}. By applying the partition coefficient $k = \dfrac{Z_S(t)}{Z_L(t)}$ the above equation can be transformed to the form

$$Z_L(t_{p+1}) = \frac{m_0\, Z_0}{k\, m_S(t_{p+1}) + m_L(t_{p+1})}. \tag{8}$$

We divide the region into control volumes V_j of length Δx_j, $j = 0, \ldots, n$. If contribution of the solid phase in volume V_j at moment t is denoted by $f_j(t)$, then the mass of metal in the solid state and liquid state contained in volume V_j at moment t is defined, respectively, by the following formulas

$$m_{S,j}(t) = V_j\, \varrho_2\, f_j(t), \tag{9}$$

$$m_{L,j}(t) = V_j\, \varrho_1\, (1 - f_j(t)). \tag{10}$$

Using the above relations, equation (8) can be written in the form

$$Z_L(t_{p+1}) = \frac{b\, \varrho_1\, Z_0}{k\, \varrho_2 \sum\limits_{j=0}^{n} \Big(\Delta x_j\, f_j(t_{p+1})\Big) + \varrho_1 \sum\limits_{j=0}^{n} \Big(\Delta x_j \left(1 - f_j(t_{p+1})\right)\Big)}, \tag{11}$$

where b denotes half of thickness of the plate (see Fig. 1).

In the inverse problem analyzed, for the known values of temperature ($(x_i, t_j) \in \Omega \times (0, t^*)$):

$$T(x_i, t_j) = U_{ij}, \qquad i = 1, 2, \ldots, N_1, \quad j = 1, 2, \ldots, N_2, \tag{12}$$

where N_1 denotes the number of sensors and N_2 represents the number of measurements taken from each sensor, our aim is to determine the value of heat transfer coefficient α. For the fixed value of heat transfer coefficient the above problem turns into a direct problem, whose solution enables finding temperature curves $T_{ij} = T(x_i, t_j)$. Using the calculated temperatures T_{ij} and the given temperatures U_{ij} we can construct the following functional describing the error of approximate solution

$$J(\alpha) = \sum_{i=1}^{N_1} \sum_{j=1}^{N_2} \big(T_{ij} - U_{ij}\big)^2. \tag{13}$$

3. Method of solution

To solve the direct Stefan problem (Eqs. (1)–(6)) alternating phase truncation method is applied [11, 23, 25]. In this method in place of temperature T we insert the enthalpy

$$H(T) = \int_0^T c(u)\,\varrho(u)\,du + \eta(T)\,L\,\varrho_2, \tag{14}$$

where

$$\eta(T) = \begin{cases} 1 & \text{for } T > T^*\big(Z_L(t)\big), \\ 0 & \text{for } T \leq T^*\big(Z_L(t)\big). \end{cases} \tag{15}$$

Function $H(T)$ is discontinuous at the point given by the temperature of phase change T^*. Its left-hand side and right-hand side limits at this point will be denoted as H_s and H_l:

$$H_s = \int_0^{T^*(Z_L(t))} c(u)\,\varrho(u)\,du, \tag{16}$$

$$H_l = H_s + L\,\varrho_2. \tag{17}$$

If we use equation (14) for Stefan problem solution, in each phase the heat conduction equation with the temperature replaced by enthalpy is obtained.

Algorithm of the alternating phase truncation method (for one time step) consists of two stages. In the first stage the entire domain is reduced to the liquid phase only, i.e. at points where the value of enthalpy is smaller than H_l such quantity of heat is supplied (symbolically) that the enthalpy takes the value of H_l. Heat transfer problem in one-phase domain, obtained in this way, can be solved using one of the known methods (for example, the finite element method), thanks to which an approximate distribution of enthalpy can be calculated. At points where a certain quantity of heat was added, the same quantity of heat must be now taken away. After this operation the distribution of enthalpy taken as the starting point for the second stage of calculations is obtained.

In the second stage the entire domain is reduced to the solid phase only, i.e. at points of the domain where the value of enthalpy is higher than H_s, such quantity of heat is taken away (symbolically) that the enthalpy becomes equal to H_s. As in the first stage, an approximate distribution of enthalpy is calculated. At the end of second stage, at the points where a certain quantity of heat was taken away, the same quantity of heat must be added now. This operation completes the second stage, that is, one step of calculations of the alternating phase truncation method (transfer from moment of time t_i to moment of time t_{i+1}).

Contribution of the solid phase in volume V_j at moment t is determined from relation

$$f_j(t) = \frac{H(x_j,t) - H_s}{H_l - H_s}, \tag{18}$$

where $H(x_j,t)$ denotes the enthalpy at point $x_j \in V_j$ at moment t (constant enthalpy in control volumes is assumed). The above relation results from the adopted numerical model [29]. Next, according to formula (11) the value $Z_L(t_{p+1})$ of concentration of the alloy component at moment t_{p+1} is calculated, which determines the new value of liquidus temperature $T^*\big(Z_L(t_{p+1})\big)$ and, in consequence, the new boundary values of enthalpy H_s and H_l.

To find the minimum of functional (13) the genetic algorithm was applied. In calculations the floating point (real) coding and the tournament selection were used. In the proposed algorithm the elitist model was also applied in which the best individual of previous generation is saved and if all individuals in the current generation are worse, then the worst individual from the current

generation is replaced with the saved best individual from the previous generation. Moreover, the arithmetical crossover and the nonuniform mutation were used [23–25]. In calculations the following values of the genetic algorithm parameters were adopted: population size $n_{pop} = 100$, number of generations $N = 100$, crossover probability $p_c = 0.7$ and mutation probability $p_m = 0.1$.

4. Numerical example

To illustrate the proposed procedure let us consider the alloy Al-Cu (2% Cu) [22, 32] for which we have: $\lambda_1 = 104$ [W/(m K)], $\lambda_2 = 262$ [W/(m K)], $c_1 = 1275$ [J/(kg K)], $c_2 = 1077$ [J/(kg K)], $\varrho_1 = 2498$ [kg/m^3], $\varrho_2 = 2824$ [kg/m^3], $L = 390000$ [J/kg], $k = 0.125$, $Z_0 = 0.02$, liquidus temperature $T^*(Z_L) = 933.37 - 259.54\, Z_L$ [K], ambient temperature $T_\infty = 298$ [K] and initial temperature $T_0 = 930$ [K]. Moreover, we take that half of thickness of the plate is equal to $b = 0.08$ [m].

In the investigated inverse problem the values of three parameters α_i, $i = 1, 2, 3$, determining the function $\alpha(t)$ describing the heat transfer coefficient need to be calculated

$$\alpha(t) = \begin{cases} \alpha_1 & \text{for } t \in [0, t_1), \\ \alpha_2 & \text{for } t \in [t_1, t_2), \\ \alpha_3 & \text{for } t \geq t_2, \end{cases} \tag{19}$$

where $t_1 = 38$ [s], $t_2 = 93$ [s]. The exact values of the sought parameters are as follows

$$\alpha_1 = 1200, \quad \alpha_2 = 800, \quad \alpha_3 = 250 \text{ [W/m}^2 \text{ K]}.$$

Solutions were sought in the following sets

$$V = \Big\{\alpha(t);\ \alpha_1 \in [1000, 1500], \alpha_2 \in [500, 1000],\ \alpha_3 \in [100, 500]\Big\}.$$

We assume that in the examined region three thermocouples ($N_1 = 3$) are located: 5, 10 and 15 mm away from the external boundary of the region. Measurements of temperature were taken every 0.1, 0.5, 1 and 5 s. In calculations the exact values of temperature and the values noised by the 1, 2 and 5% random error of normal distribution were used.

In Table 1 the results of the sought parameters α_i reconstruction are presented. It includes the results received for the exact input data and various numbers of measurement points. Calculations were made for various settings of the pseudorandom number generator. The table presents mean values (calculated for fifteen executions of the algorithm) of the determined parameters α_i, percentage relative errors of the parameters reconstruction and values of standard deviation. One can see that in each case the boundary conditions are reconstructed with the minimal error being the

Table 1. Results of the sought parameters reconstruction for the exact input data and various number of measurement points (σ – standard deviation).

α_i	Error [%]	σ	α_i	Error [%]	σ
0.1 s			0.5 s		
1199.99	0.0001	0.0890	1200.21	0.0174	0.6109
800.07	0.0084	0.3229	800.19	0.0232	0.3127
249.99	0.0048	0.0519	249.95	0.0194	0.1016
1 s			4 s		
1200.29	0.0243	1.0271	1200.70	0.0586	0.9756
800.14	0.0178	0.3163	800.27	0.0338	0.4871
249.95	0.0191	0.1312	249.88	0.0466	0.1414

consequence of the stop criterion taken in the algorithm. In case of the exact input data the maximal error of sought parameters reconstruction does not exceed the value 0.06%. Successive runs of the algorithm gave similar results, which is confirmed by the value of standard deviation. The value of standard deviation slightly increases with the decreasing number of measurement points.

Figures 2 and 3 display the errors of the sought parameters reconstruction calculated for the disturbed input data. Figure 2 presents the results received in case of temperature measurements taken every 0.1 s and every 5 s and for various disturbances of input data. Figure 3 shows the results obtained for the input data biased by the errors of values 2% and 5% and for various number of control points (temperature measurements every 0.1, 0.5, 1 and 5 s). One can see that in each case the errors of reconstruction of the boundary conditions (for biased input data) are smaller than the errors of input data. For the smallest number of measurement points and disturbances of value 1% the errors do not exceed 0.98%, for disturbances of value 2% the errors do not exceed 0.87%, whereas for disturbances of value 5% the errors do not exceed 4.46%. Increasing number of measurement points results in more precise reconstruction of the sought parameters. For example, for the biggest number of measurement points the errors are smaller than 0.09%, 0.27% and 0.31%, respectively.

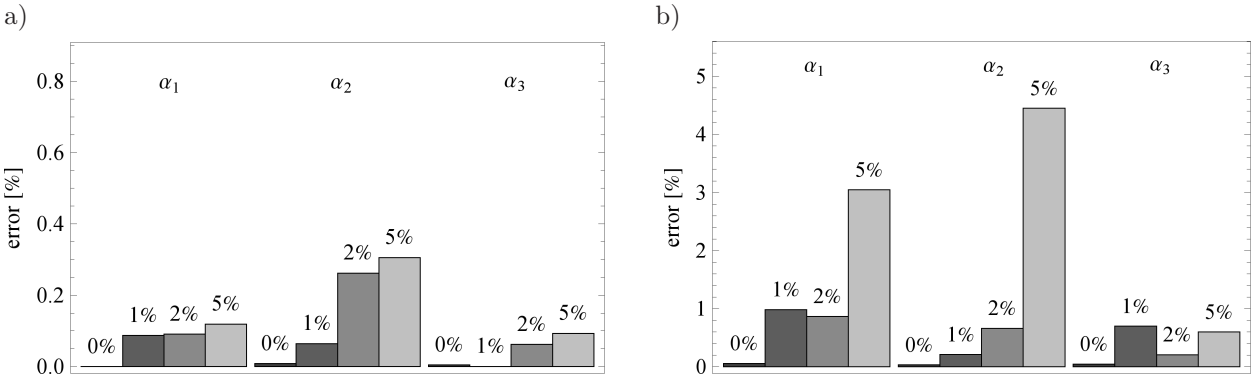

Fig. 2. Errors of heat transfer coefficient reconstruction for various errors of input data and temperature measurements taken every 0.1 s (a) and every 5 s (b).

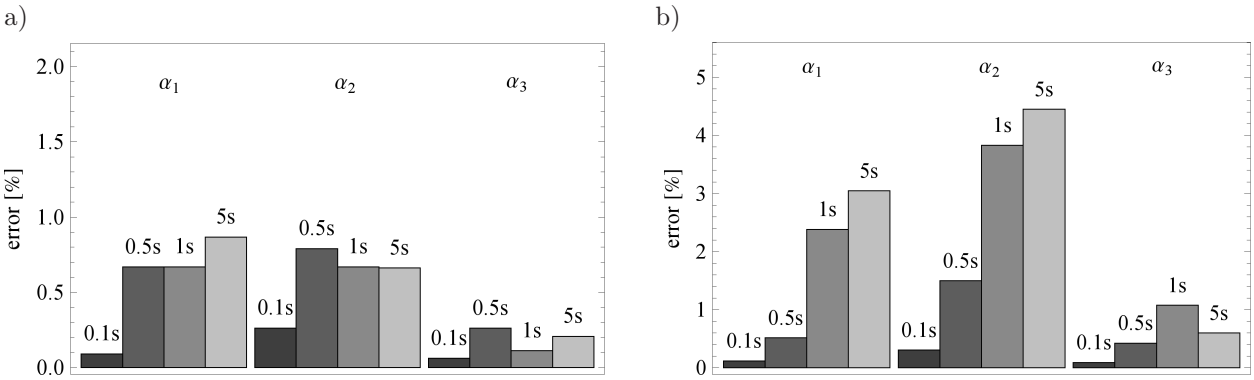

Fig. 3. Errors of heat transfer coefficient reconstruction for various number of temperature measurements (calculated for the input data biased by errors of 2% (*a*) and 5% (*b*)).

Standard deviation of the obtained results slightly increases with the decreasing number of measurement points as well as with the increasing values of the errors of input data. In case of temperature measurements taken every 0.1 s and disturbances of value 5% the standard deviation received by reconstructing parameters α_i, $i = 1, 2, 3$, is equal to 5.5034, 1.3208 and 0.6969, respectively. For temperature measurements read every 1 s the standard deviation is at the level of 13.9038, 5.6201 and 0.6905, respectively. Deviation from this rule occurred by reconstructing parameter α_1 for the temperature measurements every 5 s. Standard deviation received in this case is

equal to 1.603, the other parameters are reconstructed with the standard deviation equal to 4.5768 and 0.712, respectively.

Table 2 compiles the errors of temperature reconstruction in the control points for measurements of temperature taken every 1 s and 5 s. The presented results indicate that the temperature distribution in each case is very well reconstructed. The biggest differences between the expected and received values appear for the smallest number of measurement points and for the biggest disturbances of input data. In this situation the maximal absolute error of temperature reconstruction is at the level of 3.6634 K, whereas the mean value of absolute error is equal to 0.2832 K. Relative errors in this case are equal to, respectively, 0.3962% (maximal) and 0.032% (mean value). For the biggest number of measurements or smaller values of input data errors the discrepancies in reconstruction of temperature distribution are smaller. For example, for temperature readings made at every 0.1 s and more exact input data the errors are equal to, respectively: 0.0059 K, 0.0014 K, 0.0007 % and 0.0002 %.

Table 2. Errors of temperature reconstruction in control points for temperature measurements every 1 s and every 5 s (δ_{mean} – mean value of absolute error, $\delta_{\max}$ – maximal value of absolute error, Δ_{mean} – mean value of relative error, $\Delta_{\max}$ – maximal value of relative error).

Per.	0%	1%	2%	5%
1 s				
δ_{mean} [K]	0.0041	0.0668	0.1009	0.4963
$\delta_{\max}$ [K]	0.2686	2.8961	3.1464	3.5171
Δ_{mean} [%]	0.0005	0.0077	0.0116	0.0569
$\Delta_{\max}$ [%]	0.0290	0.3132	0.3392	0.3805
5 s				
δ_{mean} [K]	0.0135	0.1957	0.2125	0.2832
$\delta_{\max}$ [K]	0.2442	3.2796	3.2518	3.6634
Δ_{mean} [%]	0.0016	0.0224	0.0245	0.0320
$\Delta_{\max}$ [%]	0.0264	0.3536	0.3517	0.3962

5. Experimental verification

Let us present now the experimental verification of the proposed algorithm. The experimental data were obtained from the Al-Cu alloy (5% Cu) solidification process. The experiment was performed with the use of UMSA equipment. In the experiment two cylinder samples of the diameter of 18 mm and height of 20 mm each were used. The charge material was melted down in the induction crucible furnace and cast into a graphite chill-mould of the diameter of 25 mm. Next, it was mechanically worked out to adopt it to the required dimensions. In each sample the thermocouple was located in the axis of sample. The bottom and top surfaces of the samples were thermally insulated. In course of the experiment three rounds of melting and solidification of the sample material were executed.

The following values of parameters of the Al-Cu alloy (5% Cu) were taken [21, 32, 34]: $\lambda_1 = 180$ [W/(m K)], $\lambda_2 = 84$ [W/(m K)], $c_1 = 1060$ [J/(kg K)], $c_2 = 1020$ [J/(kg K)], $\varrho_1 = \varrho_2 = 2777$ [kg/m^3], $L = 386000$ [J/kg], $k = 0.17$, $Z_0 = 0.05$, ambient temperature $T_\infty = 298$ [K], initial temperature $T_0 = 1013.82$ [K] and liquidus temperature $T^*(Z_L) = 933.37 - 259.54\, Z_L$ [K].

In calculations the function α describing the heat transfer coefficient and depending on a different number of parameters was reconstructed:

$$\alpha(t) = \alpha(t; \alpha_1, \alpha_2, \ldots, \alpha_n), \qquad n \in \{1, 3, 6, 10\}.$$

To approximate the heat transfer coefficient the Bezier curves were applied [4] (in case of one parameter the heat transfer coefficient was approximated by the constant function).

The following values of parameters of the genetic algorithm were used [23–25]: population size $n_{pop} = 100$, number of generations $N \in \{100, 1000, 1500\}$, crossover probability $p_c = 0.7$, mutation probability $p_m = 0.1$ and coefficient of the nonuniform mutation $b_m = 2.0$. Number of generations was modified with the increasing number of sought parameters. Thus, in case of three parameters the number of generations was equal to 100, for six parameters it was 1000, whereas for ten parameters 1500 generations were used.

Figure 4 presents the function plot of heat transfer coefficient reconstructed for various number of sought parameters. In Table 3 there are compiled mean and maximal values of relative and absolute errors of the cooling curve reconstruction obtained using various number of sought parameters. Next, in Fig. 5 the measured cooling curve is shown and its reconstruction for six and ten parameters. Finally, Fig. 6 illustrates the influence of maximal number of generations N, used in the algorithm, on the errors of the cooling curve reconstruction.

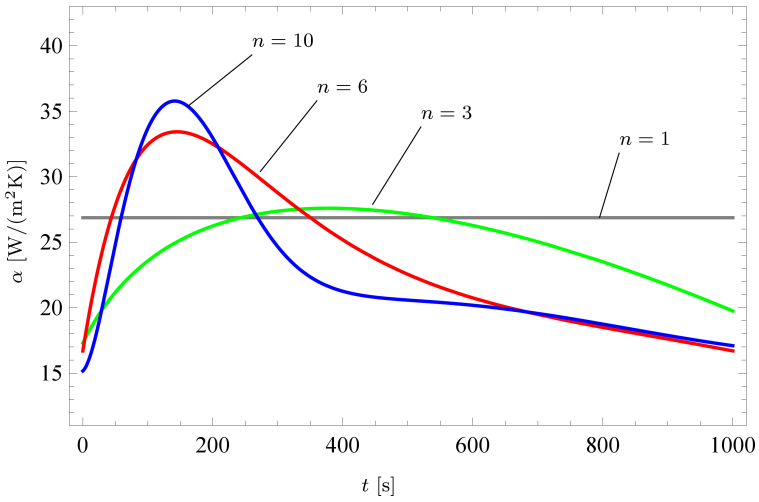

Fig. 4. Distribution of heat transfer coefficient reconstructed for various number of parameters.

Table 3. Errors of cooling curve reconstruction.

α	1	3	6	10
δ_{mean} [%]	3.892	0.797	0.438	0.235
$\delta_{\max}$ [%]	9.293	2.729	1.975	1.016
Δ_{mean} [K]	25.348	5.834	3.409	1.857
$\Delta_{\max}$ [K]	66.202	23.611	16.087	9.046

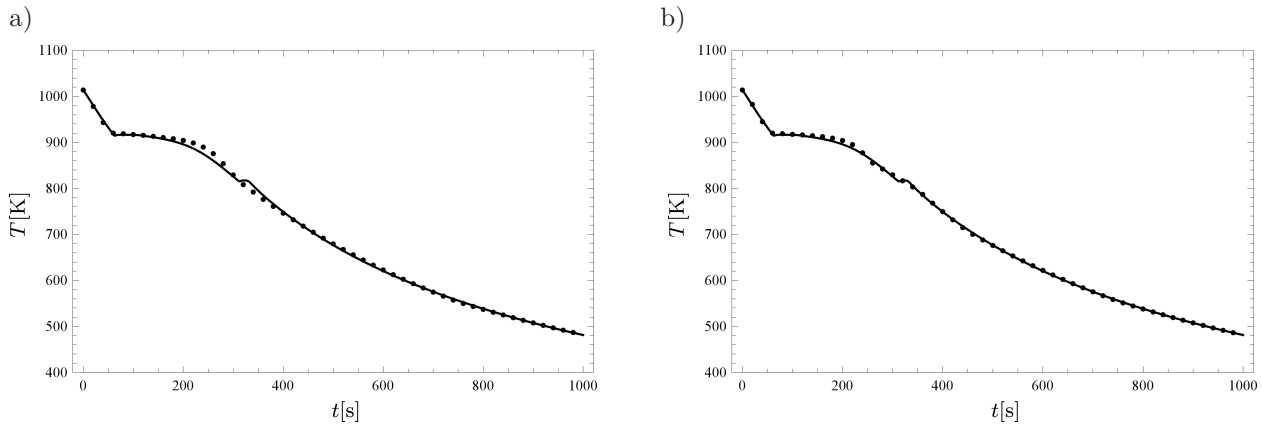

Fig. 5. Cooling curve measured (solid line) and reconstructed (points) for six (a) and ten (b) parameters.

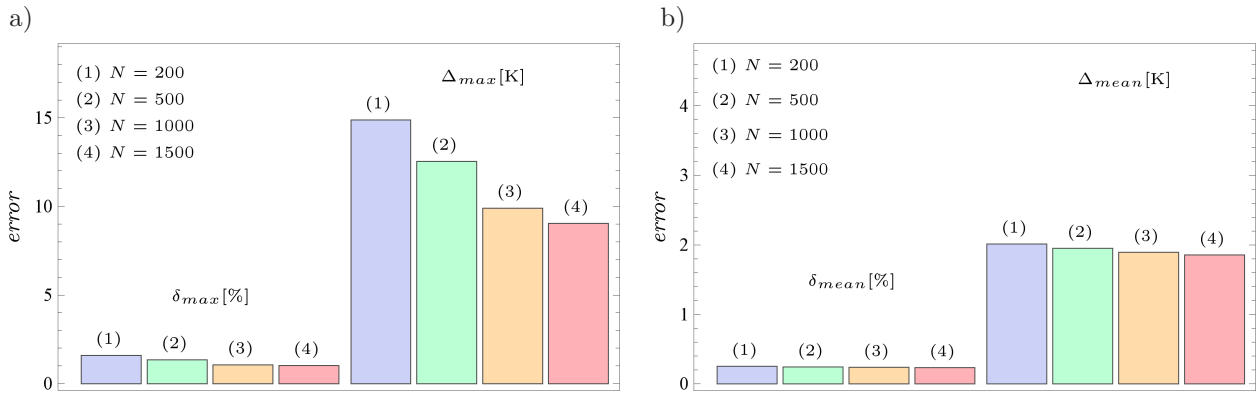

Fig. 6. Errors in reconstruction of cooling curve for ten parameters and various number of generations.

6. Conclusions

The algorithm proposed in the paper enables determination of the unknown boundary condition in the problem of binary alloy solidification. The calculations performed indicate that the reconstruction of heat transfer coefficient is very good. The presented algorithm is stable with regard to the errors of input data. The obtained results show also that the increasing number of control points or decreasing values of the input data errors lead to more precise reconstruction of the sought parameters and, in consequence, to better reconstruction of the exact temperature distribution. Experimental verification of the developed algorithm was also performed. The results indicate that the presented model, together with the algorithm, enables reconstruction of the heat transfer coefficient, which results in very good approximation of the measured values of temperature.

Acknowledgements

The authors wish to express their gratitude to Mirosława Pawlyta, Waldemar Kwaśny and Mariusz Król for their assistance in obtaining the experimental data.

References

[1] V. Alexiades, A.D. Solomon. *Mathematical Modeling of Melting and Freezing Processes*. Hemisphere Publ. Corp., Washington, 1993.
[2] A. Bokota. *Modelling of solidification and cooling of two-component metal alloys, fields of temperature, concentrations and stresses* [in Polish: *Modelowanie krzepnięcia i stygnięcia dwuskładnikowych stopów metali. Pola temperatury, stężeń i naprężeń*]. Wyd. Pol. Częstochowskiej, Częstochowa, 2001.
[3] J. Crank. *Free and Moving Boundary Problems*. Clarendon Press, Oxford, 1996.
[4] J.D. Foley, A. van Dam, S.K. Freiner, J.F. Hughes, R.L. Phillips. *Computer Graphics – Principles and Practice*. Addison-Wesley, San Diego, 1990.
[5] E. Fraś. *Crystallization of metals* [in Polish: *Krystalizacja metali*]. WNT, Warszawa, 2003.
[6] B. Ganapathysubramanian, N. Zabaras. Control of solidification of non-conducting materials using tailored magnetic fields. *J. Crystal Growth*, **276**: 299–316, 2005.
[7] B. Ganapathysubramanian, N. Zabaras. On the control of solidification using magnetic fields and magnetic field gradients. *Int. J. Heat Mass Transfer*, **48**: 4174–4189, 2005.
[8] S.C. Gupta. *The Classical Stefan Problem. Basic Concepts, Modelling and Analysis*. Elsevier, Amsterdam, 2003.
[9] W. Kapturkiewicz, E. Fraś, A.A. Burbelko. Modeling the kinetics of solidification of cast iron with lamellar graphite. *Arch. Metall. Mater.*, **54**: 369–380, 2009.
[10] W. Kurz, D.J. Fisher. *Fundamentals of Solidification*. Trans Tech Publ., Zurich, 1989.
[11] E. Majchrzak, B. Mochnacki. Application of the BEM in the thermal theory of foundry. *Eng. Anal. Bound. Elem.*, **16**: 99–121, 1995.

[12] E. Majchrzak, B. Mochnacki, J.S. Suchy. Sensitivity analysis of macrosegregation simulation with respect to partition and diffusion coefficients. *Int. J. Cast Metals Research*, **17**: 72–78, 2004.
[13] E. Majchrzak, R. Szopa. Simulation of heat and mass transfer in domain of solidifying binary alloy. *Arch. Metallurgy*, **43**: 341–351, 1998.
[14] B. Mochnacki, E. Majchrzak, R. Szopa. Simulation of heat and mass transfer in domain of casting made from binary alloy. *Arch. Foundry Eng.*, **8(4)**: 121–126, 2008.
[15] B. Mochnacki, J.S. Suchy. *Numerical Methods in Computations of Foundry Processes*. PFTA, Cracow, 1995.
[16] B. Mochnacki, J.S. Suchy. Simplified models of macrosegregation. *J. Theor. Appl. Mech.*, **44**: 367–379, 2006.
[17] B. Mochnacki, J.S. Suchy, M. Prażmowski. Modelling of segregation in the process of Al-Si alloy solidification. *Soldification of Metals and Alloys*, **2(44)**: 229–234, 2000.
[18] R. Parkitny, T. Skrzypczak. *Simulation of solidification of two-component metal alloys taking the admixture distribution under consideration* [in Polish: *Symulacja krzepnięcia dwuskładnikowych stopów metali z uwzględnieniem rozkładu domieszki*]. *Arch. Foundry*, **2(4)**: 198–203, 2002.
[19] D. Samanta, N. Zabaras. Numerical study of macrosegregation in aluminum alloys solidifying on uneven surfaces. *Int. J. Heat Mass Transfer*, **48**: 4541–4556, 2005.
[20] D. Samanta, N. Zabaras. Control of macrosegregation during the solidification of alloys using magnetic fields. *Int. J. Heat Mass Transfer*, **49**: 4850–4866, 2006.
[21] C.A. Santos, J.M.V. Quaresma, A. Garcia. Determination of transient interfacial heat transfer coefficients in chill mold castings. *J. Alloys and Compounds*, **319**: 174–186, 2001.
[22] N. Sczygiol. *Numerical modelling of thermo-mechanical phenomena in a solidifying casting and a mould* [in Polish: *Modelowanie numeryczne zjawisk termomechanicznych w krzepnącym odlewie i formie odlewniczej*]. Wyd. Pol. Częstochowskiej, Częstochowa, 2000.
[23] D. Słota. Solving the inverse Stefan design problem using genetic algorithms. *Inverse Probl. Sci. Eng.*, **16**: 829–846, 2008.
[24] D. Słota. Identification of the cooling condition in 2-D and 3-D continuous casting processes. *Numer. Heat Transfer B*, **55**: 155–176, 2009.
[25] D. Słota. Restoring boundary conditions in the solidification of pure metals. *Comput. & Structures*, **89**: 48–54, 2011.
[26] J.S. Suchy. *Segregation of alloying elements during directional solidification* [in Polish: *Segregacja pierwiastkøw stopowych podczas krzepnięcia kierunkowego*]. *Zeszyty Nauk. Pol. Śl. Mech.*, **76**: 1–132, 1983.
[27] J.S. Suchy. *Segregation of alloying elements in continuous casting technology* [in Polish: *Segregacja pierwiastków stopowych w technologii ciągłego odlewania*]. *Zeszyty Nauk. Pol. Częstochowskiej Hut.*, **19**: 169–180, 1988.
[28] J.S. Suchy, B. Mochnacki. Analysis of segregation process using the broken line model. Theoretical base. *Arch. Foundry*, **3(10)**: 229–234, 2003.
[29] R. Szopa. *Modelling of solidification and crystallization using combined boundary element method* [in Polish: *Modelowanie krzepnięcia i krystalizacji z wykorzystaniem kombinowanej metody elementów brzegowych*]. *Zeszyty Nauk. Pol. Śl. Hut.*, **54**: 1–175, 1999.
[30] V.R. Voller. A similarity solution for the solidification of a multicomponent alloy. *Int. J. Heat Mass Transfer*, **40**: 2869–2877, 1997.
[31] V.R. Voller. A numerical method for the Rubinstein binary-alloy problem in the presence of an under-cooled liquid. *Int. J. Heat Mass Transfer*, **51**: 696–706, 2008.
[32] D. Xu, Q. Li. Numerical method for solution of strongly coupled binary alloy solidification problems. *Numer. Heat Transfer B*, **20**: 181–201, 1991.
[33] G.Z. Yang, N. Zabaras. The adjoint method for an inverse design problem in the directional solidification of binary alloys. *J. Comput. Phys.*, **140**: 432–452, 1998.
[34] M. Založnik, S. Xin, B. Šarler. Verification of a numerical model of macrosegregation in direct chill casting. *Int. J. Numer. Methods Heat Fluid Flow*, **18**: 308–324, 2008.